

## Miniaturized measurement system for ammonia in air

B.H. Timmer<sup>a,\*</sup>, K.M. van Delft<sup>a</sup>, R.P. Otjes<sup>b</sup>, W. Olthuis<sup>a</sup>, A. van den Berg<sup>a</sup>

<sup>a</sup> MESA Research Institute, University of Twente, P.O. Box 217, 7500 AE Enschede, The Netherlands

<sup>b</sup> Energy Research Centre of the Netherlands (ECN), Petten, The Netherlands

Received 17 June 2003; received in revised form 11 September 2003; accepted 23 September 2003

### Abstract

The development of a miniaturized ammonia sensor made using microsystem technology is described. Gas is sampled in a sampler comprising two opposite channels separated by a gas permeable, water repellent polypropylene membrane. Subsequently, the acid sample solution is pumped into a selector where an alkaline solution is added to ionize all sampled ambient acid gasses, resulting in an enhanced selectivity. In the selector, the ammonia can diffuse through a second membrane into a purified water stream where an electrolyte conductivity sensor quantifies the resulting ammonium concentration. The realized system is shown to be selective enough not to be influenced by normal ambient carbon dioxide concentrations. Experiments with a gas flow of 3 ml/min, containing ammonia concentrations ranging from 9.8 to 0.3 ppm in a nitrogen carrier flow, into a 15  $\mu$ l/min sample solution flow and finally into a 5  $\mu$ l/min purified water stream have been carried out and show that the system is sensitive to ammonia concentration below 1 ppm.

© 2003 Elsevier B.V. All rights reserved.

**Keywords:** Gaseous ammonia sensor; Microfluidics

### 1. Introduction

In the medical community, there is a considerable interest in ammonia analyzers that can be applied to measure ammonia levels in exhaled air for the diagnosis of certain diseases [1]. Measuring breath ammonia levels can be a fast diagnostic method for patients with disturbed urea balance, e.g. due to kidney disorder [2] or *H. pylori* bacterial stomach infection [3–5]. For such applications, often only a few milliliter of exhaled air is available and, today, no suitable ammonia breath analyzer exists [6]. The ammonia analyzer should be extremely selective because the levels of ammonia are very low compared to the O<sub>2</sub> and CO<sub>2</sub> levels.

Many air ammonia detectors have been reported in literature, based on different principles [7–13]. The most sensitive and selective systems, comprising laser setups, are not suited for miniaturization and integration on a chip and are therefore not applicable for measuring in the small available gas volumes. Methods for directly measuring gas concentrations that are more suitable for miniaturization have been

shown [8–12] but most of them show poor selectivity and inadequate detection limits and are thus not suited. Other air analyzing systems make use of gas samplers, like denuders or diffusion scrubber. These systems have the advantage that they can concentrate the ammonia by sampling a volume of gas into a smaller volume of liquid, where ammonium ions are formed [14–16]. Many accurate ways to measure low ammonium concentrations have been shown [17,18].

An ambient ammonia detection system (sub-ppb level) based on this principle has been developed at the Energy Research Centre of the Netherlands (ECN) [19]. It comprises a gas sampler, a separator and a detector. First, 1 l/min gas is sampled into a 100  $\mu$ l/min acid sample solution through a microporous water repellent membrane. The used gas channel is 1.5 m long, 2 mm wide and 2 mm deep. The residence time of the gas is about 350 ms. The sample solution is pumped through the opposite channel separated from the gas channel by the membrane, that has a depth of 200  $\mu$ m. The residence time of the sample solution in the sampler is almost 360 s. The internal volume of this channel is 0.6 ml and the membrane contact area is 3000 mm<sup>2</sup>.

In the selector part, interfering acid gasses are removed and only ammonia will diffuse through a second membrane into a purified water stream. The residence time of the sample solution and the purified water are respectively 47 and

\* Corresponding author. Tel.: +31-53-489-2755;

fax: +31-53-489-2287.

E-mail address: [b.h.timmer@utwente.nl](mailto:b.h.timmer@utwente.nl) (B.H. Timmer).

URL: <http://www.bios.el.utwente.nl>.

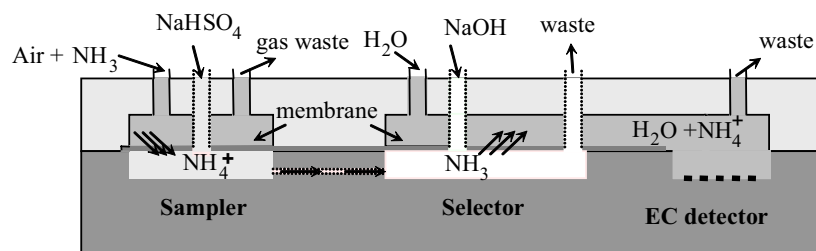


Fig. 1. Artist impression of the air ammonia analyzer developed at ECN [19] showing a gas sampler, a selector and a detector.

470 s. The resulting ammonium concentration is quantified by integrating an electrolyte conductivity sensor. The system is schematically shown in Fig. 1. A total measurement including lag time due to interconnecting tubing material requires about 20 min.

Although this apparatus requires several liters of analyte gas for detection, its principle is suited for miniaturization into a lab on a chip approach. Miniaturization of the device and integration of its key components on a chip will lead to several advantages, such as reduced energy and reagent consumption and enhanced response time. The device will be more rugged and less sensitive to disturbances [20,21]. This writing presents a hybrid miniaturized ammonia detection system based on the analyzer developed at ECN. All key components have been realized on chip to reduce internal volumes. Measurement results obtained with the system are presented.

## 2. Theory

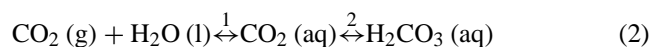
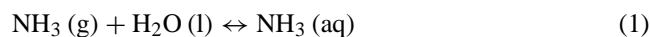
Normal ambient ammonia concentrations are in the low ppb range; an average of 2 ppb is assumed for The Netherlands [19]. The higher expected ammonia concentration for breath analysis is about 2 ppm [2]. Normal ambient CO<sub>2</sub> levels are about 300 ppm. Exhaled air can contain up to a 100-fold more, 30 000 ppm. The selectivity of the apparatus should be such that 50 ppb of ammonia is detectable [5] so the influence of 30 000 ppm of CO<sub>2</sub> should be around 2% or less of the detector signal due to 50 ppb of NH<sub>3</sub>. The following discussion will show how this is accomplished.

### 2.1. Sampler

In the gas sampler of the ammonia analyzer, a volume of gas is sampled into a smaller volume of an acidic sample solution. If there is any ammonia in the analyte gas, it will be converted to ammonium ions. In practice, ammonia is the main alkaline gas component in air. Weak acidifying gasses will hardly dissociate in the acidic environment of the sample stream. CO<sub>2</sub> is used in the following theoretical discussion because it is the most available acidifying gas in normal air.

The analyte gas is pumped through a gas channel. Opposite to this channel is a second channel where the sam-

ple solution is pumped through, separated by a water repellent/gas permeable membrane. The available gasses can diffuse through the membrane, into the solution where an equilibrium will be formed between the dissolved state and the free gaseous state in the gas channel. The reactions for ammonia and carbon dioxide are given in Eqs. (1) and (2)



The solubility of ammonia is extremely high, 27.8 mol/l at room temperature. Low concentrations of dissolved ammonia are easily converted to ammonium ions in the acidic environment in the gas sampler. Therefore it can be assumed that, when there is enough time for the ammonia to diffuse into the sample solution and the ammonia concentrations are relatively low, all gaseous ammonia will be dissolved in the sample solution. This assumption, however, cannot be made for carbon dioxide because the solubility in water is far less than for ammonia and it will only partly react with water in an acidic solution. An equilibrium between the free gaseous state and the dissolved state, both hydrolyzed and non-hydrolyzed, will form. The relation between the CO<sub>2</sub> concentration in the analyte gas expressed in its partial pressure,  $P_{\text{CO}_2}$  and the concentration in the sample solution, reaction 1 in Eq. (2), is given by Henry's law. The Henry's constant,  $S$ , for CO<sub>2</sub> at room temperature is  $9.3 \times 10^3$  Pa [22], resulting in:

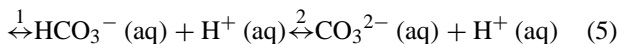
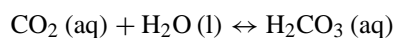
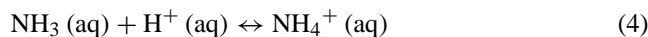
$$P_{\text{CO}_2} = S[\text{CO}_2(\text{aq})] \quad (3)$$

With an initial CO<sub>2</sub> concentration of 3%, or a partial pressure of 3000 Pa, this would result in an equilibrium dissolved CO<sub>2</sub> concentration of 1.0 mM.

Dissolved carbon dioxide will partly hydrolyzed, of which the reaction is given in reaction 2 of Eq. (2). The equilibrium constant of this reaction,  $K_{\text{h}}$ , is  $2.53 \times 10^{-3}$  M at room temperature. This means that only a small part of the dissolved CO<sub>2</sub> will be available in the hydrolyzed state. When, however, the hydrolyzed CO<sub>2</sub>, H<sub>2</sub>CO<sub>3</sub>, dissociates, new H<sub>2</sub>CO<sub>3</sub> will be formed due to the equilibrium. Therefore the total dissolved CO<sub>2</sub> concentration,  $[\text{CO}_2^*] = [\text{CO}_2(\text{aq})] + [\text{H}_2\text{CO}_3(\text{aq})]$ , is used in the rest of this discussion.

After dissolving, the gasses will react with water. This will shift the equilibrium towards an increased uptake of the

specific gas. The reactions of the two gasses are given in Eqs. (4) and (5)



The sample solution has an initial pH of 3.5. The ratio between the dissolved state and the ionized state at equilibrium can be calculated from the initial dissolved gas concentration, the initial pH and the equilibrium constant,  $K_a$ , of the reactions in Eqs. (4) and (5). Eq. (6) gives the ratio for ammonia and (7) and (8) for  $\text{CO}_2$ . When sampling carbon dioxide or ammonia, the pH will increase, shifting the equilibrium towards a lower dissociation ratio. How much influence this has on the dissociation depends on the resulting concentration levels, which on their turn depend on the ratio between the sampled gas volume and the sample solution volume

$$\frac{[\text{NH}_4^+]}{[\text{NH}_3]} = 5.5 \times 10^5 \quad (6)$$

$$\frac{[\text{HCO}_3^-]}{[\text{CO}_2^*]} = \frac{[\text{HCO}_3^-]}{[\text{CO}_2(\text{aq})] + [\text{H}_2\text{CO}_3(\text{aq})]} \quad (7a)$$

Since

$$[\text{CO}_2(\text{aq})] = \frac{1}{K_h} [\text{H}_2\text{CO}_3(\text{aq})] \quad (7b)$$

and

$$[\text{HCO}_3^-] = K_a [\text{H}_2\text{CO}_3] \frac{1}{[\text{H}^+]} \quad (7c)$$

Eq. (7a) can be solved to:

$$\frac{[\text{HCO}_3^-]}{[\text{CO}_2^*]} = \frac{K_a}{1/K_h + 1} \frac{1}{[\text{H}^+]} = 3.5 \times 10^{-6} \quad (7d)$$

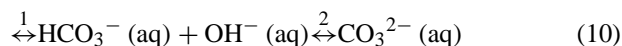
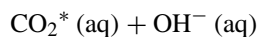
$$\frac{[\text{CO}_3^{2-}]}{[\text{HCO}_3^-]} = 1.8 \times 10^{-7} \quad (8)$$

Because the solubility of ammonia is very high, it is assumed that the ammonia flux from the gas channel through the membrane into the sample solution will be mainly towards the solution. This will even be enhanced because almost all ammonia will react with water forming ammonium ions, as shown in Eq. (6), and this reaction is very fast. The solubility of carbon dioxide is limited and in the hydrated state it will only partly dissociate, as shown in Eqs. (7d) and (8), quickly saturating the solution.

## 2.2. Selector

The sample solution is pumped into a second reaction chamber, the selector. An alkaline 0.25 M NaOH solution is added to increase the pH of the solution to 13. The equilibrium reaction shown in Eqs. (9) and (10) in an alkaline surrounding will cause the ammonium to be neutralized and

dissolved  $\text{H}_2\text{CO}_3$  to further dissociate. Since the  $\text{OH}^-$  concentration is relatively high, it is assumed no gaseous  $\text{CO}_2$  will form



The ratio between the dissolved and neutralized state of the dissolved gasses at this elevated pH can be calculated from the equilibrium constants of the reactions and the initial  $\text{OH}^-$  concentration. The base constants,  $K_b$  values, of the neutralization reaction of ammonium (Eq. (9)) and the dissociation of  $\text{H}_2\text{CO}_3$  and  $\text{HCO}_3^-$ . The  $K_h$  value of  $\text{CO}_2$  is used to calculate the equilibrium between the hydrated and non-hydrated state of dissolved  $\text{CO}_2$ . The equilibrium constant that defines the ration between  $\text{CO}_2^*$  and  $\text{HCO}_3^-$  is determined by substituting the  $\text{CO}_2$  and the  $\text{HCO}_3^-$  concentration using the  $K_h$  and  $K_b$  values, similar to the description in Eq. (7). The resulting ratios at this pH are shown in Eq. (11) for ammonia and Eqs. (12) and (13) for the reactions of  $\text{CO}_2$ :

$$\frac{[\text{NH}_3]}{[\text{NH}_4^+]} = 5.8 \times 10^3 \quad (11)$$

$$\frac{[\text{CO}_2^*]}{[\text{HCO}_3^-]} = \frac{K_b(1/K_h + 1)}{[\text{OH}^-]} = 9.1 \times 10^{-5} \quad (12)$$

$$\frac{[\text{HCO}_3^-]}{[\text{CO}_3^{2-}]} = 1.8 \times 10^{-3} \quad (13)$$

It is shown that at this pH value, most of the ammonium will be neutralized to gaseous ammonia, as shown in Eq. (11). This gaseous ammonia can diffuse through the second membrane into the purified water stream in the opposite channel. Carbon dioxide, on the other hand, will almost completely ionize, mainly to  $\text{CO}_3^{2-}$ , as shown in Eqs. (12) and (13), and is flushed with the sample solution towards the waste outlet of the system.

## 2.3. Numerical selectivity example

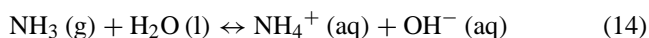
The addition of alkaline selection solution will cause an almost complete ionization of  $\text{CO}_2$ , where the ammonia will be almost completely gaseous again. As an example, the results shown in the results and discussion section of this writing are acquired with an analyte gas-sample solution ratio of 200:1. A total uptake of 50 ppb ammonia would result in an ammonium concentration in the sample solution of  $4.1 \times 10^{-7}$  M, which would not significantly influence the pH. The dissolved  $\text{CO}_2$  and the  $\text{HCO}_3^-$  concentrations would be  $1.0 \times 10^{-3}$  and  $1.4 \times 10^{-6}$  M, respectively.

In the selector the pH is increased to 13. This would result in a dissolved  $\text{NH}_3$  concentration of  $4.1 \times 10^{-7}$  M. The resulting gaseous carbon dioxide concentration at this pH

would be virtually zero. The required selectivity, less than 2% influence of 30 000 ppm CO<sub>2</sub> over 50 ppb ammonia, can be reached this way.

#### 2.4. Detector

In the detector, almost only ammonia gas is available in a purified water stream. The gaseous ammonia will partly react with water and form ions that can be detected using an electrolyte conductivity detector. The reaction that occurs is shown in Eq. (14):



The pH of the purified water stream is about 7.0. The ammonium to gaseous ammonia ratio due to the reaction with OH<sup>-</sup> can be calculated using the acid equilibrium constant. The ratio is shown in Eq. (15)

$$\frac{[\text{NH}_4^+]}{[\text{NH}_3]} = 1.7 \times 10^2 \quad (15)$$

At this pH, almost all ammonia will be ionized and therefore ammonia will continue to diffuse through the membrane into the water stream. However, the ratio will lower significantly because the pH will increase due to the dissociation of ammonia. How much this will influence the ratio depends on the actual concentration levels.

#### 2.5. Numerical sensitivity example

In the experiment described later on in this writing, a demi water flow of 1/3rd of the sample flow is used. When all ammonia gas would diffuse through the membrane into the water stream, this would result in an initial ammonia concentration of  $1.2 \times 10^{-6}$  M. The ammonium concentration at equilibrium can be calculated using Eq. (16). The initial OH<sup>-</sup> concentration due to the water equilibrium is  $10^{-7}$  M

$$K_b = 1.7 \times 10^{-5} = \frac{[\text{NH}_4^+][\text{OH}^-(\text{initial}) + \text{OH}^-]}{[\text{NH}_3(\text{initial}) - [\text{NH}_4^+]} \quad (16)$$

The ammonium concentration can be solved from this equation to be  $1.1 \times 10^{-6}$  M. The sensitivity of the ammonia analyzer is sufficient when an electrolyte conductivity sensor is used that can detect this concentration.

#### 2.6. Electrolyte conductivity detection

The conductance measured with the EC detector,  $G$  (S), depends on the electrolyte conductivity,  $K_{\text{sol}}$  (S/m), and the cell constant of the detector,  $K_{\text{cell}}$  (m<sup>-1</sup>). The electrolyte conductivity is the product of the concentrations,  $C_i$  (mol/m<sup>3</sup>), and ion conductivities,  $\lambda_i$  (S m<sup>2</sup>/mol), of all the individual types of ions in the electrolyte. This conductivity is increased when more NH<sub>4</sub><sup>+</sup> and OH<sup>-</sup> ions are formed due to an increase in sampled ammonia. The cell constant depends on the geometry of the sensor. Eq. (17) shows the expression

for the conductance,  $G$ , using the cell constant of the electrolyte detector and the conductivity of the electrolyte:

$$G = \frac{K_{\text{sol}}}{K_{\text{cell}}} = \frac{\sum_i \lambda_i C_i}{K_{\text{cell}}} \quad (17)$$

The used detector has a cell constant of 15 m<sup>-1</sup> [23]. In previous experiments it appeared to be very difficult to get cleaner water than 20 μS/m, due to interfering ion sources like in-diffusion of CO<sub>2</sub> or other polluting sources. When initially measuring in purified water and subsequently in water containing 1.1 μM of NH<sub>4</sub><sup>+</sup> and OH<sup>-</sup>, the conductivity is increased from 20 μS/m to a theoretical value of 30 μS/m due to the ammonium formation. This would cause a calculated resistance change from 400 to 267 kΩ or a conductance increase from 2.5 to 3.7 μS. With the used EC sensor, this is measurable.

### 3. Experimental

#### 3.1. Chemicals

Two types of analyte gas are used to test the miniaturized system. Pressurized air containing normal ambient CO<sub>2</sub> concentration, 0.03%, is acquired from Hoekloos. They also provided us with purified nitrogen and a mixture of 10 ppmv (±10%) ammonia in nitrogen.

The sample solution with a pH of 3.5 is made by dissolving 39 mg NaHSO<sub>4</sub>, acquired from Acros, in a litre of purified water. The alkaline selector solution is made diluting a standard 1 M NaOH solution to 0.1 M with purified water. This purified water is made in the lab in a Millipore Elix3 water purification system.

#### 3.2. Instrumentation miniaturized detection system

The system shown schematically in Fig. 1 has been realized as a hybrid miniaturized detection system. The key components, the gas sampler, the selector and the electrolyte conductivity sensor have been realized on chip. Both the gas sampler and the selector comprise two opposite channels, separated by a gas permeable water repellent membrane. PTFE and PP membranes have been tested. The original large-scale detector makes use of PTFE membranes, clamped between Perspex plates that comprise the channels. The membrane is clamped water-tight between the two plates, forming the required channel-membrane-channel structure. This is, however, not applicable on the miniaturized scale because the PTFE membrane is too compressible. Due to the applied pressure required for the sealing, the membrane will deform and clog the only several micrometer deep channels. Instead of PTFE, PP membranes are used in this experiment because PP membranes are far sturdier. PP membranes have been acquired from Schleider and Schuell (PP 0.22 μm hydrophobic membrane). One major

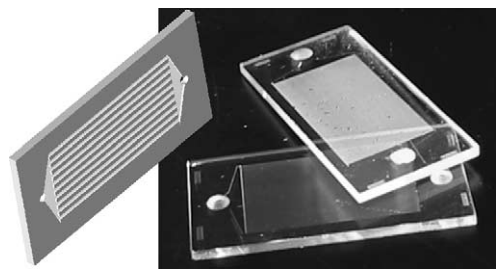


Fig. 2. Schematic and photo of the glass chips used in the separator.

other advantage is that these membranes can be glued to glass using epoxy glue.

Channel structures have been etched into glass using wet chemical etching. Borofloat glass wafers are first cleaned in fuming nitric acid. A chromium mask layer is deposited and structured using standard photolithography and wet chromium etching. Subsequently 15  $\mu\text{m}$  deep channels are etched in the glass in a 10% HF solution. The used photoresist is stripped from the wafer in acetone. Through-holes are made using powder blasting [24]. A photosensitive protective foil is laminated onto the wafer and structured using photolithography and developed in sodium carbonate. After powder blasting the through-holes with 9  $\mu\text{m}$  aluminum oxide powder the foil is stripped in sodium carbonate and the wafer is ultrasonically cleaned in acetone to remove powder residue and diced. A photo of the realized glass chips is shown in Fig. 2. The chips comprise of 45 channels with a length of 20 mm and a width of 100  $\mu\text{m}$ , with an internal volume of 1.35  $\mu\text{l}$ . The total membrane contact area is 90  $\text{mm}^2$ . Compared to the macroscale device, the sample solution volume to surface area ratio is decreased by a factor of 10, which is beneficial for reducing diffusion times.

Two chips are pressed together with a PP membrane in between that was cut the same size as the chips. Epoxy glue is applied to the side of the chips. The glue will be pulled between the stack by capillary forces. By applying a minimal amount of glue, the wafers are sealed together without glue flowing into the channels.

A miniaturized EC detector optimized for measuring low ion concentrations in small volumes has been realized in previous research [23]. A comb structured, two electrodes, con-

ductivity detector with 95 electrodes with a width of 10  $\mu\text{m}$ , a length of 1270  $\mu\text{m}$  and a spacing between the electrodes of 30  $\mu\text{m}$  has been realized, resulting in a cell constant of 15  $\text{m}^{-1}$ .

After cleaning a Pyrex glass wafer, a negative image of the designed electrode structure is created on the wafer in photoresist using standard photolithography. After sputtering a chromium adhesion layer, a platinum electrode layer is sputtered over the entire wafer. The electrode structure is realized using a lift-off step, by ultrasonically removing the photoresist layer.

A silicon wafer is used to make the channel structure and through-holes to connect the EC sensor to the rest of the system. Channels are made in silicon by standard photolithography and reactive ion etching. Through-holes are made using powder blasting in the same way as is done with the glass wafers. The glass wafer with the electrodes on it is anodically bonded to the silicon wafer in an EV-501 anodic bonder and subsequently diced into chips. A photo of a realized chip comprising two EC detectors is shown in Fig. 3.

The chips are interconnected by gluing the through-holes onto each other. A Perspex T-splitter specially fabricated for this purpose is glued between the gas sampler and the selector to create an inlet for the NaOH solution.

### 3.3. Measurement procedure

A 3 ml/min analyte gas flow is applied to the gas sampler. With a gas channel volume of 1.5  $\mu\text{l}$ , this results in a residence time of 30 ms. Gas flow was controlled using mass flow controllers from Bronkhorst Hightech, EL-flow F-110C. The mass flow controllers have a maximum flow of 3 ml/min with a minimum controllable flow of 2%, which is 60  $\mu\text{l}/\text{min}$ . Both the ammonia and the nitrogen source should always be open, at least at 2%, to prevent in-diffusion of  $\text{CO}_2$  into the tubing (30 cm of PTFE tubing, 0.8 mm ID, 1.6 mm OD), reducing the maximum and minimum attainable ammonia concentration to 9.8 and 0.2 ppm, respectively. The dried air contains 300 ppm  $\text{CO}_2$ , and is used for selectivity testing.

A 325  $\mu\text{M}$   $\text{NaHSO}_4$  sample solution, with a pH of 3.5, is pumped through the gas sampler at 15  $\mu\text{l}/\text{min}$  using a

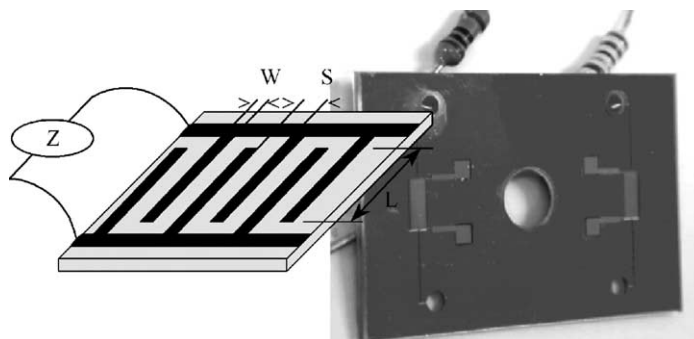


Fig. 3. Schematic and photo of the EC detector.



syringe pump, CMA 102 microdialysis pump. The residence time of the solution in the gas sampler is 6 s. The same pump is used to add a 0.25 M NaOH solution to the selector at a flow rate of 3  $\mu\text{l}/\text{min}$ . The residence time of the mixture in the selector will be about 5 s. Pre-cleaned de-ionized water was purified by an ion exchange column filled with Baker mixed bed ion exchange resin and pumped directly into the selector at a flow rate of 5  $\mu\text{l}/\text{min}$ . The EC detector was connected to the liquid outlet of the selector by directly gluing the chips together so that the through-holes connect and to home-made interface electronics to measure the conductivity of the sample liquid after gas sampling. The total flow-through time of the purified water is about 40 s.

#### 4. Results and discussion

The first experiment conducted with the total system is a selectivity test. Once the system became stable using pressurized air, the gas source is changed to pure nitrogen. There is no significant change in conductivity, as can be seen in Fig. 4. Although it is hard to give a number for the selectivity from this measurement, it is clear from the results the system does not respond to normal ambient  $\text{CO}_2$  concentration levels.

It should be noticed that the conductivity of the purified water is much higher than theoretically can be expected. Apparently, the water is contaminated during the experiment. This might be caused by diffusion of  $\text{CO}_2$  directly into the water stream. The disadvantage of this higher conductivity baseline is the loss in detection limit. A second drawback of the current system is clogging of gas bubbles inside the EC detector. When the system is cleaned prior to the experiments by flushing through with purified water, still gas bubbles stick to the electrodes. This causes an offset in the conductivity that reduces the reproducibility of the system. Future work should focus on designing the electrodes such that it is easier to remove gas bubbles from the system.

A second conducted experiment is a sensitivity test. A nitrogen carrier gas with different ammonia concentrations is used as the analyte gas. The system is first stabilized by using the higher ammonia concentration, 9.8 ppm. Once the

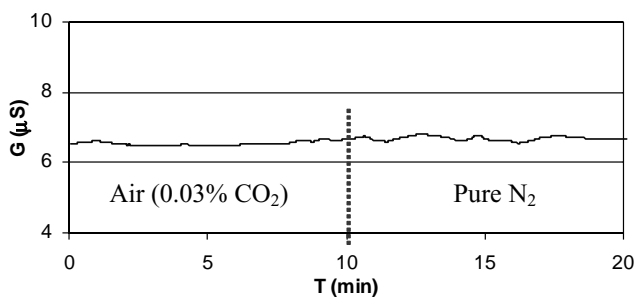


Fig. 4. Conductivity measurement curve showing no noticeable response on a change from 300 to 0 ppm  $\text{CO}_2$ .

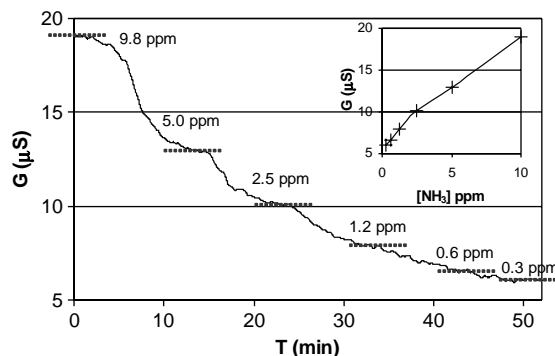


Fig. 5. Conductivity measurement curve showing sensitivity of the system to 5.0–0.5 ppm.

system got stable, the ammonia concentration is reduced from 9.8 to 5.0, 2.5, 1.2, 0.6 and 0.3 ppm, respectively. The conductivity measurement result is shown in Fig. 5.

It is shown clearly that the conductivity is increased under influence of the ammonia in the analyte gas. A higher ammonia concentration results in a higher conductivity, as expected from the theory. Unfortunately, the baseline of the conductivity, at no ionizable gas, is too high to be able to detect ammonia concentration that lie well below 1 ppm. Further optimization of the system is required to reach the 50 ppb goal. When the expected conductance is calculated from the described theory, it is clear that the measured conductance response is about a factor of 3 lower than it should be. We think this is caused by a non-optimal gas uptake in the sampler. This can be optimized by increasing the time available for the gas to diffuse through the membrane, e.g. increasing the gas channel depth. This will be optimized in further research.

The response time of the system is about 10 min. This is far more than the 60 s required for flowing through the internal volumes of the chips. Most of this time for the current system is the flow-through time through the interconnecting material and the mixer between the gas sampler and the selector/detector part that is used as the inlet for the alkaline selector solution. The total sample solution volume inside the chips is 2.7  $\mu\text{l}$ . The volume of one connector used to connect the chips to the mixer has an internal volume of 7.6  $\mu\text{l}$ , of which two are used. The mixer has an internal volume of 6.3  $\mu\text{l}$ . This implies that 89% of the internal sample solution volume is for transportation of fluids only, resulting in a response time of about 10 min. The speed of the system would significantly increase when all parts would be integrated into one system, without interconnecting tubing. This was not possible with the current system due to gluing problems.

#### 5. Conclusions

A hybrid miniaturized ammonia sensor has been realized by gluing polypropylene membranes between two glass chips comprising micromachined channels. A gas sampler

and a selector have been realized in such a way that the uptake of ammonia is enhanced and sampled acid gas is isolated into a waste stream. An electrolyte conductivity sensor is used to quantify the resulting ammonium concentration in a purified water stream.

Although further optimization of the design is required to be able to measure ppb levels of ammonia, the described ammonia detection system is shown to be selective enough to not be influenced by normal ambient CO<sub>2</sub> concentrations. Also, the system is shown to be sensitive to less than 1 ppm of ammonia.

### Acknowledgements

This research project was financially supported by STW, the Dutch funding agency for university research. The authors gratefully acknowledge the technical support from Koen van Delft and Wabe Koelmans on the realization of the chips and Ad Sprenkels for developing the interface electronics. We thank Jan Eijkel and Sven Timmer for their theoretical assistance.

### References

- [1] W. Ament, J.R. Huizenga, E. Kort, T.W. van der Mark, R.G. Grevink, G.J. Verkerke, *Int. J. Sports Med.* 20 (1999) 71.
- [2] L.R. Narasimhan, W. Goodman, C. Kumar, N. Patel, *Proc. Nat. Acad. Sci. USA* 98 (2001) 4617.
- [3] B. Marshall, J.R. Warren, *Lancet* 1 (1993) 1273.
- [4] J.C.E. Underwood, Churchill Livingstone, 2nd ed., 1996, p. 414.
- [5] D.J. Kearney, T. Hubbard, D. Putnam, *Dig. Dis. Sci.* 47 (11) (2002) 2523.
- [6] E. Verpoorte, *Electrophoresis* 23 (2002) 677.
- [7] S.G. Buckley, C.J. Damm, W.M. Vitovec, L.A. Sgro, R.F. Sawyer, C.P. Koshland, D. Lucas, *Appl. Opt.* 37 (1998) 8382.
- [8] R.K. Sharma, P.C.H. Chan, Z. Tang, G. Yan, I.-M. Hsing, J.K.O. Sin, *Sens. Actuators B* 81 (2001) 9.
- [9] F. Zee, J.W. Judy, *Sens. Actuators B* 72 (2001) 120.
- [10] M. Aslam, V.A. Chaudhary, I.S. Mulla, S.R. Sainkar, A.B. Mandale, A.A. Belhekar, K. Vijayamohanan, *Sens. Actuators A* 75 (1999) 162.
- [11] I. Laehdesmaeki, A. Lewenstam, A. Ivaska, *Talanta* 43 (1996) 125.
- [12] V.V. Chabukwar, S. Pethkar, A.A. Athawale, *Sens. Actuators B* 77 (2001) 657.
- [13] J. Maier, *Sens. Actuators B* 65 (2000) 199.
- [14] P.K. Simon, P.K. Dasgupta, Z. Vecera, *Anal. Chem.* 63 (1991) 1237.
- [15] P.F. Lindgren, P.K. Dasgupta, *Anal. Chem.* 61 (1989) 19.
- [16] C.B. Boring, R. Al-Horr, Z. Genfa, P.K. Dasgupta, *Anal. Chem.* 74 (2002) 1256.
- [17] G. Schultze, C.Y. Liu, M. Brodowski, O. Elsholz, *Anal. Chim. Acta* 214 (1988) 121.
- [18] R.M. Tiggelaar, T.T. Veenstra, R.G.P. Sanders, E. Berenschot, H. Gardeniers, M. Elenspoek, A. Prak, R. Mateman, J.M. Wissink, A. van den Berg, *Sens. Actuators B* 92 (2003) 25.
- [19] J.W. Erisman, R. Otjes, A. Hensen, P. Jongejan, P.V.D. Bulk, A. Khlystov, H. Möls, S. Slanina, *Atm. Environ.* 35 (2001) 1913.
- [20] A. van den Berg, T.S.J. Lammerink, *Topics Curr. Chem.* 194 (1997) 21.
- [21] A. Manz, N. Graber, H.M. Widmer, *Sens. Actuators B* 1 (1990) 244.
- [22] R. Chang, University Science Books, 3rd ed., Chapter 11, 2000.
- [23] B.H. Timmer, W. Sparreboom, W. Olthuis, P. Bergveld, A. van den Berg, *Lab on Chip* 2 (2002) 121.
- [24] H. Wensink, M.C. Elwenspoek, *Sens. Actuators A* 102 (2002) 157.